

Gravitational Redshift Test with the Space Radio Telescope “RadioAstron”

A. V. Biriukov¹, V. L. Kauts^{1,2}, V. V. Kulagin³, D. A. Litvinov^{3*}, and V. N. Rudenko³

¹*Astro Space Center, Lebedev Physical Institute, Moscow, Russia*

²*Bauman Moscow State Technical University, Moscow, Russia*

³*Sternberg Astronomical Institute, Moscow State University, Moscow, Russia*

Received May 12, 2014; in final form, May 21, 2014

Abstract—The space radio telescope “RadioAstron” is equipped with a high performance hydrogen maser frequency standard and thus provides a unique opportunity for a gravitational redshift test. We consider various modes of operation of the on-board scientific equipment and their impact on accuracy of the anticipated experiment. We find that the accuracy of the test is limited by $\sim 10^{-2}$ for the hardware configuration routinely used in radio astronomical observations, which is a consequence of using ballistic data to remove the nonrelativistic Doppler frequency shift from the analyzed signal. On the other hand, the so-called “Semi-coherent” mode of the on-board hardware provides for combining the space and ground maser signals in such a way that the resulting signal carries information about the useful effect but is free from the nonrelativistic Doppler and tropospheric frequency shifts. The proposed compensation scheme, which is different from the one used in the Gravity Probe A experiment, allows for testing the gravitational redshift effect with $\sim 10^{-6}$ accuracy.

DOI: 10.1134/S1063772914110018

1. INTRODUCTION

According to the Einstein Equivalence Principle (EEP), an electromagnetic wave propagating in a region of space with nonuniform gravitational potential experiences a gravitational frequency shift [1, 2], proportional to the gravitational potential difference ΔU between the measurement points and the frequency f of the wave:

$$\frac{\Delta f_{\text{grav}}}{f} = \frac{\Delta U}{c^2}. \quad (1)$$

The effect can also be phrased in the language of time interval differences ΔT , measured by clocks situated at the corresponding locations:

$$\frac{\Delta T_{\text{grav}}}{T} = \frac{\Delta U}{c^2}. \quad (2)$$

The first reliable gravitational redshift test was conducted in 1960 by Pound and Rebka [3] (see also [4]) in a laboratory experiment based on the Moessbauer effect. The most precise test of (1) to date was performed in the Gravity Probe A experiment (GP-A) of 1976 [5], in which the frequencies of two hydrogen masers were compared—one on the Earth and the other on board a rocket with a ballistic

trajectory of 10^4 km apogee. The experiment confirmed Eq. (1) to 1.4×10^{-4} accuracy.

The interest in conducting even more precise tests of (1) and (2) is motivated by the search for violation of the EEP, predicted by the majority of Grand Unification Theories. The mechanisms of violation can be different but, in any case, they result in a non-universal coupling of the graviton to the other particles. This, in effect, results in a modification of Eq. (1), which, in the case of two frequency standards a and b under gravitational potentials U_a and U_b , takes the following form:

$$\frac{\Delta f_{\text{grav}}}{f} = \frac{U_a}{c^2}(1 + \varepsilon_X^{(a)}) - \frac{U_b}{c^2}(1 + \varepsilon_X^{(b)}), \quad (3)$$

where $\varepsilon_X^{(a)}$ and $\varepsilon_X^{(b)}$ are the violation parameters, which may depend both on composition X of the source of the gravitational field and the quantum transitions used in the respective frequency standards. At the same time, Eq. (3) states that a result of a physical experiment depends on a space-time point where the experiment is performed. Therefore, the gravitational redshift experiment is a direct test of the Local Position Invariance part of the EEP. (Note, however, that, according to Schiff’s conjecture (see monograph [2]), any violation of this symmetry implies that the other two parts of the EEP, i.e. the Weak Equivalence

*E-mail: litvirq@yandex.ru

Principle and the Local Lorentz Invariance, are also violated.)

In the case of two identical frequency standards Eq. (3) simplifies to:

$$\frac{\Delta f_{\text{grav}}}{f} = \frac{\Delta U}{c^2} (1 + \varepsilon_X^{(a)}). \quad (4)$$

Thus the GP-A experiment set the limit for $\varepsilon_{\oplus}^{(H)}$, which characterizes the violation of (1) for the hydrogen hyperfine transition and the Earth as a source of the gravitational field: $\varepsilon_{\oplus}^{(H)} = (0.05 \pm 1.40) \times 10^{-4}$.

Several experiments aimed at improving the currently achieved accuracy of the test by 2–4 orders of magnitude are to be conducted in the near future. The European Space Agency’s ACES mission [6] intends to install two atomic clocks, an H-maser and the caesium fountain clock PHARAO [7], onto the International Space Station. The active phase of the mission had been put off several times and currently is being scheduled for 2016. Because of the ISS’s low orbit, the gravitational potential difference between the ground and the on-board clocks will be only $\approx 10\%$ of that possible with a spacecraft at a distance of $\gtrsim 10^5$ km from the Earth. Nevertheless, PHARAO’s accuracy, which is expected to reach $\sim 10^{-16}$ in microgravity, provides for measurement accuracy of ε at the level of 10^{-6} .

Another european initiative is STE-QUEST [8], a candidate mission for the ESA Cosmic Vision M4 programme, with a goal to test (1) with 10^{-7} – 10^{-8} accuracy in the gravitational field of the Earth. Additionally, a special choice of the orbit, which will allow the spacecraft to simultaneously communicate with tracking stations at different continents, will provide for testing (1) in the field of the Sun. The accuracy of this type of experiment, not requiring a frequency standard on board the spacecraft, is speculated to reach $\sim 10^{-6}$. The question of the mission’s frequency standard has not settled by the time of writing. The launch is to occur no earlier than 2026.

Finally, an experiment with a potential of testing the redshift effect (1) in the field of the Earth with $\sim 10^{-6}$ accuracy is currently being carried out as a part of the mission of the space radio telescope (SRT) “RadioAstron” with participation of the authors of the present paper. The possibility for this experiment came with the decision to add a space hydrogen maser (SHM) frequency standard to the scientific payload of the mission’s spacecraft. Because of the impossibility to reconstruct the orbit with an accuracy needed for this experiment, a modification of the communications subsystem of the spacecraft was suggested, which would have provided for online compensation

of the contributions of the nonrelativistic Doppler effect and the troposphere in the analyzed signal (the “Cronos” project). The main point of the modification was to allow for independent synchronization of the Earth-spacecraft-Earth two-way link to a ground hydrogen maser (GHM) frequency standard, while the spacecraft-Earth one-way link be synchronized to the SHM. Unfortunately, the proposed modification did not materialize. The modes of the high-data-rate radio complex (HDRRC) do not allow to independently synchronize the frequencies of the links used for transmission of tone signals, i.e., 7.2 GHz (up) and 8.4 GHz (down), and the 15 GHz carrier of the data downlink (used for observational and telemetry data transmission).

It is possible, however, to independently synchronize the carrier (15 GHz) and the modulation (72 or 18 MHz) frequency of the data downlink. This mixed, or “Semi-coherent,” mode of synchronization hasn’t been used in astronomical observations so far. As our analysis shows, for this mode it is possible to devise a compensation scheme, which is similar to the one used by the GP-A experiment, and which results in the contributions of the nonrelativistic Doppler effect and the troposphere eliminated in its output signal. The accuracy of the experiment based on this compensation scheme can reach the limit 1.8×10^{-6} , set by the frequency instability and accuracy of the SHM.

The article is organized into 6 sections. In the second section we give a general account of a practical approach to gravitational redshift tests with spaceborne atomic frequency standards and also derive expressions, which can be used to estimate accuracy of such experiments. In the third section we describe some characteristics of the SRT “RadioAstron” hardware, which are important for the gravitational experiment, and, in particular, discuss the three main modes of the on-board hardware synchronization. In the fourth section we consider the perspectives of an experiment utilizing the “H-maser” mode, which is routinely used in astronomical observations, and also present some results of our analysis of relevant experimental data. The fifth section is devoted to the mixed, or “Semi-coherent” mode of synchronization. The sixth section summarizes our investigations and outlines the prospects for future work.

2. EXPERIMENT CONCEPT AND ACCURACY

Gravitational redshift experiments with spacecrafts (SC), having atomic time and frequency standards on board, can be based either upon frequency (1) or time interval (2) comparisons. The GP-A experiment followed the frequency approach, ACES will utilize both, and STE-QUEST is going

to rely only on the frequency one. Both approaches are possible for the SRT “RadioAstron,” but because of the on-board and ground hardware peculiarities, the frequency method promises a potentially higher accuracy, so we will discuss it exclusively. We will also limit our discussion to the case of comparing only two frequency standards of the same type, one at a SC and another at a ground tracking station (TS).

In order to compare the output frequencies of a ground f_e and a space-borne f_s atomic standards, one needs to transmit any (or both) of these signals by means of radio or optical links. The comparison thus becomes complicated by the necessity of extracting a small gravitational frequency shift from the mix of accompanying effects, such as resulting from the relative motion of the SC and the TS or signal propagation through media with non-uniform and time-varying refractive indices. The total frequency shift of a signal, propagating from the SC to the TS, is given by the following equation:

$$f_s^\downarrow = f_s + \Delta f_{\text{grav}} + \Delta f_{\text{kin}} + \Delta f_{\text{instr}} + \Delta f_{\text{media}}, \quad (5)$$

where f_s^\downarrow is the frequency of the signal, as received by and measured at the TS, Δf_{grav} is the gravitational frequency shift, Δf_{kin} is the frequency shift due to the SC and TS relative motion, Δf_{media} is the propagation media contribution (ionospheric, tropospheric, interstellar medium), Δf_{instr} encompasses various instrumental effects, which we will not consider here. Now, Eq. (5) can be used to determine the gravitational frequency shift Δf_{grav} . Indeed, f_s^\downarrow is measured at the TS, Δf_{kin} can be evaluated from the orbital data (assuming special relativity is valid), Δf_{media} can be found from multi-frequency measurements (for the ionospheric and interstellar media contributions) and meteorological observations (for the tropospheric one), estimation of Δf_{instr} involves calibration of the hardware and a study of the transmitting, receiving and measuring equipment noise. The value of f_s is unobservable and, therefore, presents a certain difficulty. It is convenient to express it in terms of the frequency of the ground-based standard f_e and an offset Δf_0 :

$$f_s^\downarrow = f_e + \Delta f_{\text{grav}} + \Delta f_{\text{kin}} + \Delta f_{\text{instr}} + \Delta f_{\text{media}} + \Delta f_0, \quad (6)$$

where

$$f_s = f_e + \Delta f_0. \quad (7)$$

The problem of f_s (or Δf_0) being not measurable directly has different solutions depending on the type of the frequency standards used and the possibility of varying the gravitational potential difference ΔU between them (see Section 3).

In order to test (1) it is also necessary to determine the value of U , which can be calculated from models of the gravitational potential of the Earth [9] and the Solar System [10] and implies precise knowledge of the geographical coordinates of the TS and the orbit of the SC. An important point here is that the orbit reconstruction algorithm should not at any point make an assumption of validity of (1).

Let us now consider the problem of the experiment accuracy estimation. A general expression for the error of measurement of the general relativity violation parameter ε can be obtained by varying (4):

$$\delta\varepsilon = \frac{\delta \frac{\Delta f_{\text{grav}}}{f}}{\frac{\Delta U}{c^2}} - \frac{\frac{\Delta f_{\text{grav}}}{f}}{\left(\frac{\Delta U}{c^2}\right)^2} \delta \frac{\Delta U}{c^2}. \quad (8)$$

The error $\delta \frac{\Delta U}{c^2}$ is usually comparable to or less than $\delta \frac{\Delta f_{\text{grav}}}{f}$. Therefore, we can use Eq. (4) with $\varepsilon = 0$ here and obtain

$$\delta\varepsilon \approx \frac{\delta \frac{\Delta f_{\text{grav}}}{f} - \delta \frac{\Delta U}{c^2}}{\frac{\Delta U}{c^2}}. \quad (9)$$

At long distances the contribution $\delta \frac{\Delta U}{c^2}$ can be completely ignored, if the purpose of the experiment is to achieve accuracy $\delta\varepsilon \sim 10^{-6}$. Indeed, the error due to inaccurate knowledge of the ground maser coordinates is a constant, e.g. for $\delta r_e = 10$ cm equal to

$$\delta U_e/c^2 = 1.1 \times 10^{-17}. \quad (10)$$

The error $\delta U_s/c^2$ falls off as $\propto r_s^{-2}$ for δr_s fixed. So, in case of $\delta r_s = 100$ m, then at $r_s > 10^5$ the error $\delta\varepsilon < 4 \times 10^{-17}$. Thus, when $r_s > 10^5$ km and the desired accuracy $\delta\varepsilon \sim 1 \times 10^{-6}$, we can use

$$\delta\varepsilon \approx \frac{\delta \frac{\Delta f_{\text{grav}}}{f}}{\frac{\Delta U}{c^2}}. \quad (11)$$

Obviously, (11) is valid at arbitrary distances if the SRT coordinates are determined accurately enough.

Some specifications of the on-board H-maser of the SRT “RadioAstron”

Stability (Allan deviation) $\sigma_y(\tau)$:	
$\tau = 1000$ s	3×10^{-15}
$\tau = 1$ h	2×10^{-15}
Accuracy $\frac{\Delta f}{f}$	3×10^{-13}
Drift at:	
1 day	1×10^{-15}
1 year	2×10^{-13}

Note, that Eqs. (8), (9), and (11) give the error of ε for a single measurement of the signal’s total gravitational frequency shift Δf_{grav} due to the gravitational potential difference ΔU . The case when only the varying part of the redshift effect is determined, which is possible with eccentric SC orbit, and also the case of repeated measurements are considered below in the course of the discussion of the gravitational redshift experiment with the SRT “RadioAstron.”

3. SOME IMPORTANT CHARACTERISTICS OF THE SRT “RADIOASTRON” HARDWARE

The cornerstone piece of the SRT hardware for the gravitational experiment of the type considered here is the space hydrogen maser frequency standard. Some of the relevant performance parameters of this device are given in the Table.

The SHM output signal is transmitted to a TS by the above-mentioned HDRRC [11], which includes two transmitters at 8.4 and 15 GHz, and a 7.2 GHz receiver. The frequencies of the signals used both by the HDRRC transmitters and the radio-electronics science complex (RESC), can be synthesized either from the reference signal of the SHM or from the 7.2 GHz output of the on-board receiver, which receives the signal transmitted by the TS and locked to the ground H-maser. The mode of the on-board hardware synchronization significantly affects not only the achievable accuracy but the very possibility of the gravitational redshift experiment.

3.1. The “H-Maser” Mode

The main synchronization mode used in radio astronomical observations is the combination of the

“H-maser” mode of the HDRRC and “Use HDRRC-1” of the RESC, or, for short, the “H-maser” mode. In this mode the SHM signal is used to synchronize both the HDRRC and the RESC. The frequency f_s of the signal, transmitted by the HDRRC, and its frequency f_s^\downarrow , as received at a TS, are related by the following equation [12] (cf. Eq. (5)):

$$f_s^\downarrow = f_s \left(1 - \frac{\dot{D}}{c} - \frac{v_s^2 - v_e^2}{2c^2} + \frac{(\mathbf{v}_s \cdot \mathbf{n})^2 - (\mathbf{v}_e \cdot \mathbf{n}) \cdot (\mathbf{v}_s \cdot \mathbf{n})}{c^2} + \frac{\Delta f_{\text{grav}}}{f} + \frac{\Delta f_{\text{trop}}}{f} \right) + \Delta f_{\text{ion}} + o\left(\frac{v}{c}\right)^2, \quad (12)$$

where $\dot{D} = (\mathbf{v}_s - \mathbf{v}_e) \cdot \mathbf{n}$ is the radial velocity of the SRT relative to the TS, \mathbf{v}_s and \mathbf{v}_e are the velocities of the SRT and the TS, respectively, \mathbf{n} is a unit vector, pointing in the direction opposite to the one of the signal propagation, Δf_{grav} is the gravitational redshift, Δf_{ion} and Δf_{trop} are the ionospheric and tropospheric frequency shifts; all kinematical values are referred to a geocentric inertial reference frame.

The various terms at the r.h.s. of (12) are grouped so as to make it obvious that the kinematical, gravitational and tropospheric contributions are proportional to the transmitted signal frequency, while the ionospheric contribution is inversely proportional to it [13]. The availability of the 2-frequency link provides for accurate estimation of the ionospheric term [12], but the contributions of the other effects cannot be separated from each other and need to be calculated from ballistic data. As we will see in the next section, this causes a large error of the Doppler effect $\frac{\dot{D}}{c}$ determination and thus degrades the experiment accuracy to $\sim 1\%$.

3.2. The “Coherent” Mode

Let us now consider the “Coherent” mode of the on-board hardware synchronization, also known as the phase-locked loop mode. Here a sinusoidal signal of 7.2 GHz frequency, synchronized to the GHM, is sent to the SRT, where it is received by the HDRRC and used to lock the frequencies of the RESC. All the signals transmitted to the TS by the HDRRC are also phase-locked to the received 7.2 GHz signal: the 8.4 GHz tone, the 15 GHz carrier of the data transfer link, and, lastly, its 72 (or 18) MHz modulation frequency. A signal radiated by the TS with frequency f_e has the following frequency on return from the SC

$$\begin{aligned}
(Rf_e^\uparrow)^\downarrow = & Rf_e \left(1 - \frac{\dot{D}_{12}}{c} - \frac{\dot{D}_{23}}{c} + \frac{\dot{D}_{12} \cdot \dot{D}_{23}}{c^2} \right. \\
& + \frac{(\mathbf{v}_s \cdot \mathbf{n}_{23})^2 + (\mathbf{v}_{e1} \cdot \mathbf{n}_{12})^2 - (\mathbf{v}_s \cdot \mathbf{n}_{12})(\mathbf{v}_{e1} \cdot \mathbf{n}_{12}) - (\mathbf{v}_{e3} \cdot \mathbf{n}_{23})(\mathbf{v}_s \cdot \mathbf{n}_{23})}{c^2} \\
& \left. + \frac{\Delta f_{\text{trop}12}}{f} + \frac{\Delta f_{\text{trop}23}}{f} \right) + \Delta f_{\text{ion}12} + \Delta f_{\text{ion}23} + o\left(\frac{v}{c}\right)^2, \quad (13)
\end{aligned}$$

where $R = 8.4/7.2$ for the 8.4 GHz downlink or $R = 15/7.2$ for the 15 GHz one, $\dot{D}_{12} = (\mathbf{v}_s - \mathbf{v}_{e1}) \cdot \mathbf{n}_{12}$, $\dot{D}_{23} = (\mathbf{v}_s - \mathbf{v}_{e3}) \cdot \mathbf{n}_{23}$, and the other designations are obvious from Fig. 1.

The ‘‘Coherent’’ mode alone is of no interest to the redshift experiment, because, as obvious from (13), the received signal has no information about the gravitational redshift effect. However, in the case of simultaneous operation of the one- (12) and two-way (13) links, their signals can be combined by means of a special radio engineering compensation scheme [12], which outputs a signal containing information about the gravitational redshift but, at the same time, free from the 1st-order Doppler and tropospheric contributions. (It is also possible to compensate for the ionosphere but only in case of a special selection of the ratios of the up- and downlink frequencies.) This compensation scheme, first used in the GP-A mission, cannot be applied in the case of ‘‘RadioAstron,’’ because, as mentioned above, the mode of independent synchronization of the carrier frequencies of the HDRRC links is not supported.

3.3. The ‘‘Semi-coherent’’ Mode

It is possible, however, to synchronize the 8.4 and 15 GHz frequencies of the HDRRC transmitters to the GHM-locked 7.2 GHz tone (the ‘‘Coherent’’ mode of HDRRC), while the RESC is synchronized to any of the on-board frequency standards (the ‘‘Use on-board frequency standard 1 or 2’’ mode of the RESC). This ‘‘Semi-coherent’’ mode turns out to be the most suitable for the gravitational experiment. Indeed, just like in the ‘‘Coherent’’ mode, the net gravitational redshift is cancelled in the received 8.4 GHz tone and in the carrier of the 15 GHz data link. However, in contrast to the ‘‘Coherent’’ mode, the modulation frequency of the data link is locked not to the 7.2 GHz uplink but to the SHM signal, hence all components of the data link signal spectrum, except for the carrier, are influenced by the gravitational effect. There’s an issue, though, in that the magnitude of the gravitational shift is then proportional to the modulation frequency 72 (or 18) MHz, whereas all the

disturbing effects still occur at the GHz scale of the carriers. At first sight, this should lead to ≈ 100 -fold degradation of the measurement accuracy, as compared to the GP-A approach where the SHM signal was encoded directly in the spacecraft downlink tone. However, as will be shown below, the compensation scheme can be arranged in such a way that all disturbing effects are transferred to the modulation frequency scale too. Moreover, just like in GP-A, it turns out to be possible to eliminate the contributions of the 1st-order Doppler and tropospheric effects as well.

4. MEASURING THE GRAVITATIONAL REDSHIFT IN THE ‘‘H-MASER’’ MODE

Let us now consider testing the gravitational redshift effect in the case when the ‘‘RadioAstron’s’’ on-board hardware is operating in the ‘‘H-maser’’ mode. The main equation of this mode is (12), wherein it is convenient to use (7) to express the SHM frequency f_s in terms of the GHM frequency f_e and the frequency offset Δf_0 . Note that for ‘‘RadioAstron’s’’ orbit

$$\frac{\dot{D}}{c} < 3 \times 10^{-5}, \quad (14)$$

and that Δf_0 does not exceed the frequency standard’s accuracy $\frac{\Delta f_0}{f} < 3 \times 10^{-13}$ (see the table above). So,

$$\begin{aligned}
f_s^\downarrow = & f_e \left[1 - \frac{\dot{D}}{c} - \frac{v_s^2 - v_e^2}{2c^2} \right. \\
& + \frac{(\mathbf{v}_s \cdot \mathbf{n})^2 - (\mathbf{v}_e \cdot \mathbf{n}) \cdot (\mathbf{v}_s \cdot \mathbf{n})}{c^2} + o\left(\frac{v}{c}\right)^2 \left. \right] \\
& + \Delta f_0 + \Delta f_{\text{grav}} + \Delta f_{\text{ion}} + \Delta f_{\text{trop}}, \quad (15)
\end{aligned}$$

where, according to the above remarks, the largest of the neglected terms is less than $\frac{\Delta f_0 \dot{D}}{f_e c} < 10^{-17}$.

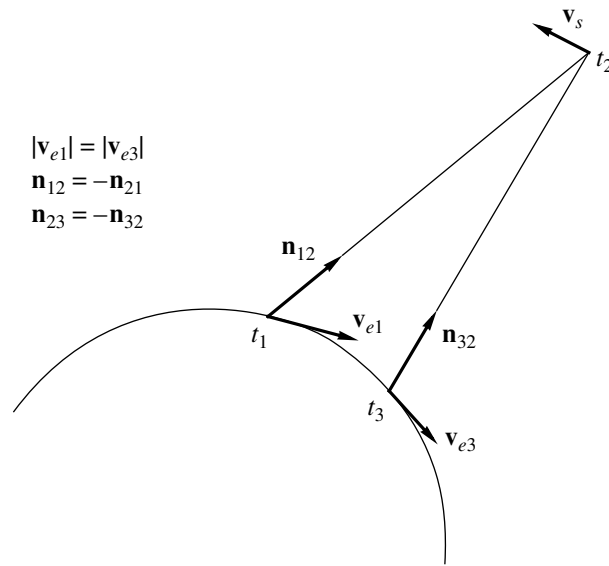


Fig. 1. The SRT and TS kinematics.

Obviously, if we determine Δf_{grav} from (15), its accuracy will be limited by the unknown value of the offset Δf_0 . When Δf_0 is believed to be small enough, one can use (15) directly to estimate the frequency offset of the SHM relative to the GHM due to gravitation (the so-called absolute measurement approach). For example, the accuracy of the above-mentioned PHARAO fountain clock, when installed at the ISS, is expected to reach $\left(\frac{\Delta f_0}{f_e}\right)_{\text{PHARAO}} \sim 1 \times 10^{-16}$, while the effect to be measured is

$$\frac{U_e - U_{\text{ISS}}}{c^2} = \frac{GM}{c^2} \left(\frac{1}{r_e} - \frac{1}{r_{\text{ISS}}} \right) = 4.3 \times 10^{-11}. \quad (16)$$

Using (11) we see that in this case the ε parameter cannot be determined with an accuracy better than

$$\delta \varepsilon_{\text{ACES}} \sim 2 \times 10^{-6}. \quad (17)$$

Now consider the case of “RadioAstron.” For the

SRT at apogee ($r_{\text{ap}} \sim 3 \times 10^5$ km) the gravitational potential difference is substantially larger:

$$\frac{U_e - U_{\text{ap}}}{c^2} = \frac{GM}{c^2} \left(\frac{1}{r_e} - \frac{1}{r_{\text{ap}}} \right) = 6.8 \times 10^{-10}, \quad (18)$$

but, because of the H-maser’s much poorer accuracy (see the table above), the accuracy of the absolute measurement of the gravitational redshift with “RadioAstron” is limited to

$$\delta \varepsilon_{\text{RA,ap}} \sim 4 \times 10^{-4}, \quad (19)$$

which is both worse than (17) and does not exceed the GP-A result.

It may be reasonable to test (1) not by way of determining the total value of the gravitational redshift, but rather its variation while the SRT is moving along its orbit. Using (15) and (7) we can calculate the difference of the frequency measurements performed at the TS at instants t_1 and t_2 :

$$\begin{aligned} f_{s1}^\perp - f_{s2}^\perp &= (f_{s1} - f_{s2}) \\ + f_e \left[-\frac{\dot{D}_1 - \dot{D}_2}{c} - \frac{v_{s1}^2 - v_{s2}^2}{2c^2} + \frac{(\mathbf{v}_{s1} \cdot \mathbf{n}_1)^2 - (\mathbf{v}_e \cdot \mathbf{n}_1) \cdot (\mathbf{v}_{s1} \cdot \mathbf{n}_1) - (\mathbf{v}_{s2} \cdot \mathbf{n}_2)^2 + (\mathbf{v}_e \cdot \mathbf{n}_2) \cdot (\mathbf{v}_{s2} \cdot \mathbf{n}_2)}{c^2} \right. \\ &\quad \left. + o\left(\frac{v}{c}\right)^2 \right] + (\Delta f_{\text{grav}1} - \Delta f_{\text{grav}2}) + (\Delta f_{\text{ion}1} - \Delta f_{\text{ion}2}) + (\Delta f_{\text{trop}1} - \Delta f_{\text{trop}2}). \end{aligned} \quad (20)$$

The Moon’s gravitational field causes the apogee

and perigee of the SRT to slowly evolve. The most

favorable periods for the gravitational experiment are such that the perigee height is at minimum, i.e., the winter–spring periods of 2014 and 2016, when it is equal to $\sim 1.5 \times 10^3$ km, so that

$$\left(\frac{U_{\text{ap}} - U_{\text{per}}}{c^2} \right)_{\text{max}} = 5.5 \times 10^{-10}. \quad (21)$$

During the least favorable period (winter–spring of 2015) the perigee is at $\sim 65 \times 10^3$ km height, so that

$$\left(\frac{U_{\text{ap}} - U_{\text{per}}}{c^2} \right)_{\text{min}} = 5.3 \times 10^{-11}.$$

The term $f_{s1} - f_{s2}$ in (20) is the frequency drift of the SHM over $t_2 - t_1$ time. In general, H-masers drift substantially over large time intervals, i.e., in amount comparable to their accuracy (see the table). The drift per-day, however, is usually quite small. For “RadioAstron’s” SHM

$$\left(\frac{f_{s1} - f_{s2}}{f} \right)_{\text{1 day}} \sim 1 \times 10^{-15}. \quad (22)$$

This value should be compared to the frequency instability of the SRT at the time of 1000 s, which is a realistic duration of a gravitational redshift session:

$$\sigma_y(\tau) = 3 \times 10^{-15} \quad \text{at} \quad \tau = 1000 \text{ s}. \quad (23)$$

Approximately one day is needed for the SRT to travel from perigee to a distance where the gravitation potential is almost equal to its value at apogee. Therefore, the accuracy of a single modulation-type experiment is limited not by the frequency drift (22) of either the SHM or the GHM (of the same order) but by the H-maser frequency instability (23). The accuracy of this test can be obtained from (11) by the substitutions $\Delta f_{\text{grav}} \rightarrow \Delta f_{\text{grav1}} - \Delta f_{\text{grav2}}$ and $U_s - U_e \rightarrow U_{\text{ap}} - U_{\text{per}}$. So, taking into account only the frequency standards’ instability (23) and the value of the gravitational potential modulation (21), we obtain the following *limit for the total accuracy of a single experiment* to determine the value of the gravitational redshift modulation in the favorable period of low perigee:

$$\delta\varepsilon > 5.5 \times 10^{-6}. \quad (24)$$

For the least favorable period of high perigee we have $\delta\varepsilon > 5.6 \times 10^{-5}$.

The important advantage of the “RadioAstron” mission, as compared to GP-A, lies in the possibility of conducting the experiment multiple times. Statistical accumulation of measurement results provides for reduction of the random error contributions by a factor of \sqrt{N} , where N is the number of measurements performed. For $N \sim 10$, in particular, the contribution (23) of the frequency instability becomes equal to the one of the frequency drift. Since the

drift causes a systematic error, accumulating data any further will not improve the experiment accuracy. Assuming that the drift of the SHM relative to the GHM cannot be measured to better than (22), we arrive at the following *limit for the accuracy of the modulation-type gravitational redshift experiment* with “RadioAstron”:

$$\delta\varepsilon > 1.8 \times 10^{-6}. \quad (25)$$

In practice, the accuracy of the experiment under discussion is limited not by the instability or accuracy of the frequency standards, but by insufficiently accurate knowledge of the SRT orbit. Let us suppose, for example, that the spacecraft radial velocity is determined with error $\delta\dot{D} = 3$ mm/s, the error of the gravitational frequency shift, obtained from (20), is

$$\text{then } \delta \frac{\Delta f_{\text{grav}}}{f} = 1.0 \times 10^{-11}.$$

In this case, obviously, there is no sense in determining only the modulation part of the redshift effect, because the error due to the frequency standard’s accuracy is 2 orders of magnitude smaller. The total value of the redshift, according to (11) and (18), can be determined with error $\delta\varepsilon = 1.5 \times 10^{-2}$.

The frequency measurements of the 8.4 and 15 GHz downlinks are performed at the Greenbank and Puschino TSs on regular basis during the SRT observational sessions. Fig. 2 presents some results of our analysis of the 8.4 GHz signal frequency measurements, performed at the Puschino TS during the period of October 5–16, 2012. The data reduction is based on (15), the kinematic parameters are calculated from the reconstructed orbit of the SRT, the ionospheric contribution is recovered from the dual 8.4 and 15 GHz frequency measurements [12], the tropospheric one is estimated by using meteorological data and mapping functions [14]. In order to check the experimental data quality, we let $\Delta f_{\text{grav}}/f = \Delta U/c^2$ and plot the frequency residuals calculated as a difference between the measured and calculated values of the received frequencies. We observe that the rms frequency residual is 0.18 Hz, which is equal to $\approx 3\%$ of the total gravitational shift of the 8.4 GHz signal at that epoch (5.3–5.7 Hz). If we make a reasonable assumption that general relativity is not violated at this level, then, according to (11), the obtained value gives a lower limit of the experiment accuracy $\delta\varepsilon$. If we suppose that this error comes mainly from the uncertainty in the radial velocity, then $\delta\dot{D} \sim 6$ mm/s.

5. MEASURING THE GRAVITATIONAL REDSHIFT IN THE “SEMI-COHERENT” MODE

The advantage of the “Semi-coherent” mode over the “H-maser” one lies in the possibility of construct-

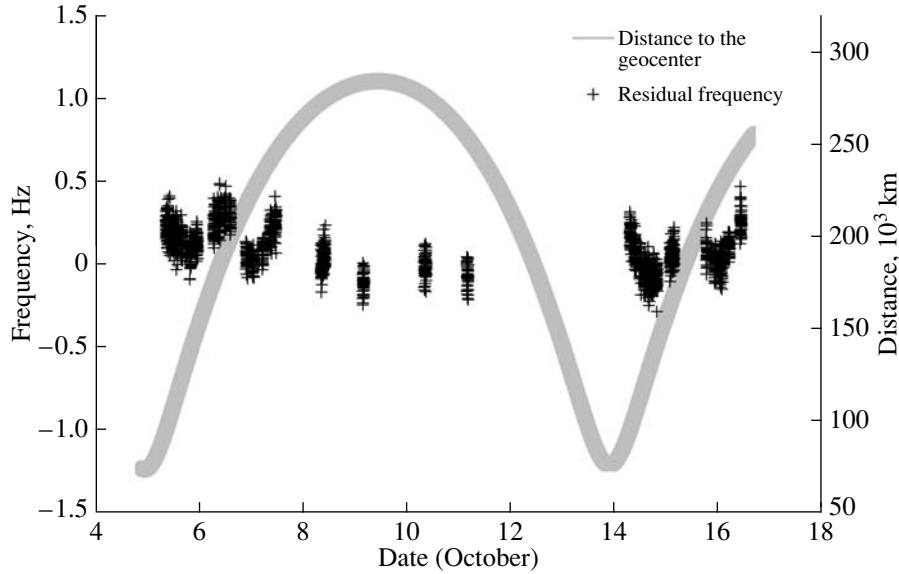


Fig. 2. Residual frequency of the 8.4 GHz signal, October 2012. Effects taken into account: Doppler (1st and 2nd order), gravitational frequency shift, ionosphere, troposphere.

ing a compensation scheme, which would synthesize a signal containing the desired gravitational frequency shift but not the contributions of the nonrelativistic Doppler and the troposphere. This relaxes the requirements to the accuracy of orbital reconstruction and, therefore, provides for attaining a record value of the accuracy of the gravitational redshift test $\delta\varepsilon \sim 10^{-6}$. In what follows we discuss how a signal with the specified properties could be synthesized from the signals of the 15 GHz downlink and the GHM.

As we noted earlier, the “Semi-coherent” mode implies that the 7.2 GHz tone, transmitted by a TS to the SRT, is used to generate the frequencies of the SRT RESC and, by effective multiplication by $8.4/7.2$ and $15/7.2$, of the 8.4 GHz tone and the 15 GHz carrier of the SRT-TS data downlink. The modulation frequency of the 15 GHz channel, as opposed to the “Coherent” mode, is generated from the SHM signal.

Let us discuss in some more detail the frequency conversions of the signals which they experience in the course of their “up” and “down” trips. The frequency f_e^\uparrow of the signal, received by the SRT, is related to its frequency f_e , as transmitted by the TS, according to:

$$f_e^\uparrow = f_e \left[1 - \frac{\dot{D}_{12}}{c} + \frac{\Delta f_{\text{grav}12}}{f} - \frac{v_{e1}^2 - v_s^2}{2c^2} + \frac{(\mathbf{v}_{e1} \cdot \mathbf{n}_{12})^2 - (\mathbf{v}_s \cdot \mathbf{n}_{12}) \cdot (\mathbf{v}_{e1} \cdot \mathbf{n}_{12})}{c^2} + T_{12} + \frac{1}{f_e^2} I_{12} + o\left(\frac{v}{c}\right)^2 \right], \quad (26)$$

where, in contrast to the similar Eq. (12), here we explicitly give the frequency dependence of the ionospheric and tropospheric contributions: $\frac{\Delta f_{\text{trop}}}{f} = T_{12}$, $\frac{\Delta f_{\text{ion}}}{f} = \frac{I_{12}}{f^2}$. It is assumed that T and I are constants in f for the frequency range 7–15 GHz, but may depend upon the moment of time and the signal propagation path [13].

The 7.2 GHz signal, after it has been received by the SRT and its frequency multiplied by $R = 15/7.2$, serves as a carrier for the SRT-to-TS data communications link. Data is sent using QPSK-coding with a modulation frequency of 72 (or 18) MHz, locked to the SHM. The spectrum of the 15 GHz signal, as received at a TS, gets distorted as a result of various propagation effects. According to (12), a spectrum component with frequency $Rf_e^\uparrow \pm \nu_s$ is seen at the TS shifted to

$$(Rf_e^\uparrow \pm \nu_s)^\downarrow = (Rf_e^\uparrow \pm \nu_s) \times \left[1 - \frac{\dot{D}_{23}}{c} + \frac{\Delta f_{\text{grav}23}}{f} - \frac{v_s^2 - v_{e3}^2}{2c^2} + \frac{(\mathbf{v}_s \cdot \mathbf{n}_{23})^2 - (\mathbf{v}_{e3} \cdot \mathbf{n}_{23}) \cdot (\mathbf{v}_s \cdot \mathbf{n}_{23})}{c^2} + T_{23} + \frac{1}{(Rf_e^\uparrow \pm \nu_s)^2} I_{23} + o\left(\frac{v}{c}\right)^2 \right]. \quad (27)$$

Note, that since the ionospheric term is dispersive, we have $(Rf)^\downarrow \neq Rf^\downarrow$, $(f + \nu)^\downarrow \neq f^\downarrow + \nu^\downarrow$ and similarly for the “ \uparrow ” superscript.

Now we put (26) into (27), taking into account that $\phi_{e3} = \phi_{e1} = \phi_e$ and $v_{e3}^2 = v_{e1}^2 = v_e^2$ (which is justified for the time intervals of order of signal light times), and, expanding in the small parameters ν/Rf and $(Rf^\uparrow - Rf)/Rf \approx (\dot{D}_{12}/c)/Rf$, we obtain:

$$\begin{aligned} & (Rf_e^\uparrow \pm \nu)^\downarrow - (Rf_e^\uparrow)^\downarrow \\ &= \pm \nu_s \left(1 - \frac{\dot{D}_{23}}{c} + \frac{\Delta f_{\text{grav}23}}{f} - \frac{v_s^2 - v_e^2}{2c^2} \right. \\ & \left. + \frac{(\mathbf{v}_s \cdot \mathbf{n}_{23})^2 - (\mathbf{v}_{e3} \cdot \mathbf{n}_{23}) \cdot (\mathbf{v}_s \cdot \mathbf{n}_{23})}{c^2} + T_{23} \right) \\ & \mp \frac{I_{23}}{Rf} \frac{\nu}{Rf} + \Delta\nu_0 + o\left(\frac{\nu}{c}\right)^2. \end{aligned} \quad (28)$$

It is important to note, that for the differential signal (28), as opposed to (27), all the corrections are proportional to the narrow-band modulation frequency ν_s . However, this signal has no advantage over signal (12) of the ‘‘H-maser’’ mode, since it still includes the 1st-order Doppler effect contribution. Comparing Eqs. (28) and (12), we also observe that the signs of the ionospheric terms in them are opposite.

Let us now consider the following combination of the frequency components of the 15 GHz signal:

$$\begin{aligned} & \left\{ \left[(Rf_e^\uparrow + \nu_s)^\downarrow - (Rf_e^\uparrow)^\downarrow \right] - \nu_e \right\} \\ & - \frac{1}{2} \frac{\nu_0}{Rf_0} \left[(Rf_e^\uparrow)^\downarrow - Rf_e \right]. \end{aligned} \quad (29)$$

The subscript ‘‘0’’ denotes the nominal values of the modulation frequency and the carrier, i.e., $\nu_0 \equiv 72$ MHz and $f_0 \equiv 15$ GHz. We introduce them here because of the considerations of a practical realization of the compensation algorithm (see below). In the case of an online compensation by a radio engineering scheme (hardware approach) the factor $\frac{\nu_0}{Rf_0}$ translates into a multiplication factor of a frequency synthesizer. In the case of a software-based approach this value is represented by a numerical constant in the program code. (In the latter case the following expression can be used instead of (29): $\left\{ \left[(Rf_e^\uparrow + \nu_s)^\downarrow - (Rf_e^\uparrow)^\downarrow \right] - \nu_0 \right\} - \frac{1}{2} \frac{\nu_0}{Rf_0} \left[(Rf_e^\uparrow)^\downarrow - Rf_0 \right]$.)

The nominal and actual frequency values are related to each other by the equations similar to (7):

$$f_s = f_0 + \tilde{\Delta}f_0, \quad \nu_s = \nu_0 + \tilde{\Delta}\nu_0, \quad (30)$$

where, in general, $\Delta f_0 \neq \tilde{\Delta}f_0$. Obviously, actual signal frequencies should not deviate from their nominal values by more than the frequency standard’s

accuracy. In particular, for ‘‘RadioAstron’’ (see the table),

$$\tilde{\Delta}f_0/f < 3 \times 10^{-13}, \quad \tilde{\Delta}\nu_0/\nu < 3 \times 10^{-13}. \quad (31)$$

Let us now deal with Eq. (29), putting into it (28), (27) with $\nu = 0$, and the following expansions, which are valid up to order $\Delta t = |\mathbf{r}_s - \mathbf{r}_{e3}|/c$,

$$\mathbf{v}_{e1} \approx \mathbf{v}_{e3} - 2\Delta t \cdot \mathbf{a}_{e3}, \quad (32)$$

$$\mathbf{n}_{12} \approx \mathbf{n}_{32}$$

$$+ \frac{2\Delta t}{|\mathbf{r}_s - \mathbf{r}_{e3}|} [\mathbf{v}_{e2} - \mathbf{n}_{32} \cdot (\mathbf{n}_{32} \cdot \mathbf{v}_{e3})], \quad (33)$$

where \mathbf{a}_{e3} is the TS acceleration at time t_3 . Then, using (7), (30), and (14), we obtain:

$$\begin{aligned} & \left\{ \left[(Rf_e^\uparrow + \nu_s)^\downarrow - (Rf_e^\uparrow)^\downarrow \right] - \nu_e \right\} \\ & - \frac{1}{2} \frac{\nu_0}{Rf_0} \left[(Rf_e^\uparrow)^\downarrow - Rf_e \right] = \nu_e \left[\frac{\Delta f_{\text{grav}23}}{f} \right. \\ & \left. - \frac{|\mathbf{v}_s^2 - \mathbf{v}_e^2|}{2c^2} + \frac{\mathbf{a}_{e3} \cdot \mathbf{n}_{32} \Delta t}{c} + \frac{1}{2} (T_{23} - T_{12}) \right] \\ & - \frac{3}{2} \frac{I_{23}}{Rf_0} \frac{\nu_0}{Rf_0} - \frac{1}{2} \frac{I_{12}}{f_0} \frac{\nu}{f_0} \\ & + \Delta\nu_0 + o(\nu/c)^2 + o(\Delta t), \end{aligned} \quad (34)$$

where we dropped several terms like $\frac{I_{23}}{Rf} \frac{\nu}{Rf} \frac{\dot{D}_{12}/c}{f}$ and $\frac{I}{f} \frac{\Delta\nu_0}{f}$.

The signal (34) is free from the 1st-order Doppler effect contribution. Moreover, since $T_{12} \approx T_{23}$ up to small-scale and rapid tropospheric fluctuations, the contribution of the troposphere is almost zero too. The signal (34) is, therefore, identical in these two respects to the output signal of the GP-A compensation scheme. However, the approximate equality $I_{12} \approx I_{23}$ does not result in the cancellation of the ionospheric term here. Note, that we can compose a combination with a property of the 1st-order Doppler and tropospheric terms cancelled not only from the central and a side component of the signal spectrum but also from any two symmetrical components $Rf^\uparrow + \nu$ and $Rf^\uparrow - \nu$. It is easy to show that in this case, too, the ionospheric term persists. This fact turns out to be a consequence of the sign change of the ionospheric term in (34), and it can be shown that no combination of the 15 GHz signal’s spectral components results in the cancellation of the ionospheric contribution, even if it were possible, like in GP-A, to select the frequency ratios of the links beforehand.

For a practical application of Eq. (34), or a similar one with symmetrical side components, the spectrum

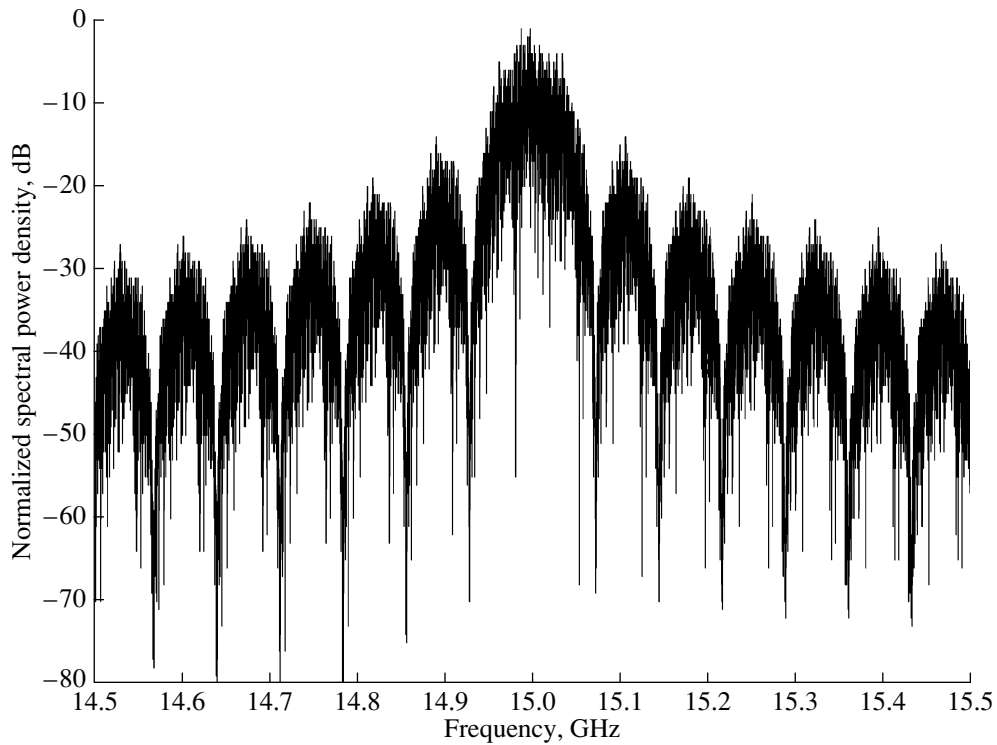


Fig. 3. 15 GHz signal spectrum modelling. Transmitted data is noise-like (white and gaussian).

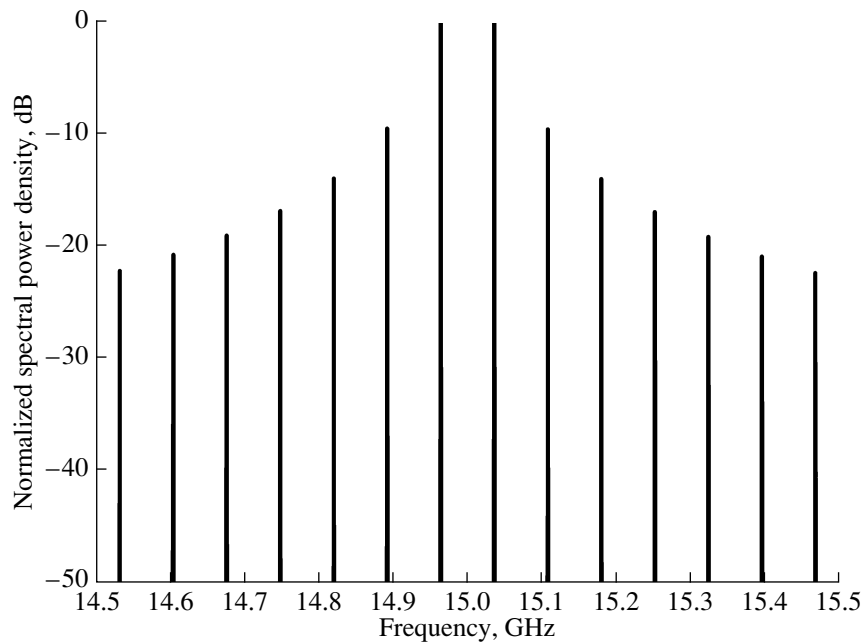


Fig. 4. 15 GHz signal spectrum modelling. Transmitted data is 010101...

of the QPSK-modulated 15 GHz signal should contain isolated peaks with high signal-to-noise ratio. In reality, when transmitting astronomical observations data, which are of stochastic nature, the signal spectrum, on the contrary, looks like a series of wide

“caps” (Fig. 3), so their maxima cannot be easily located. The desired form of the spectrum can be achieved by transmitting a regular data pattern of alternating 0 s and 1 s. The “RadioAstron” on-board formatter can be switched into a test mode

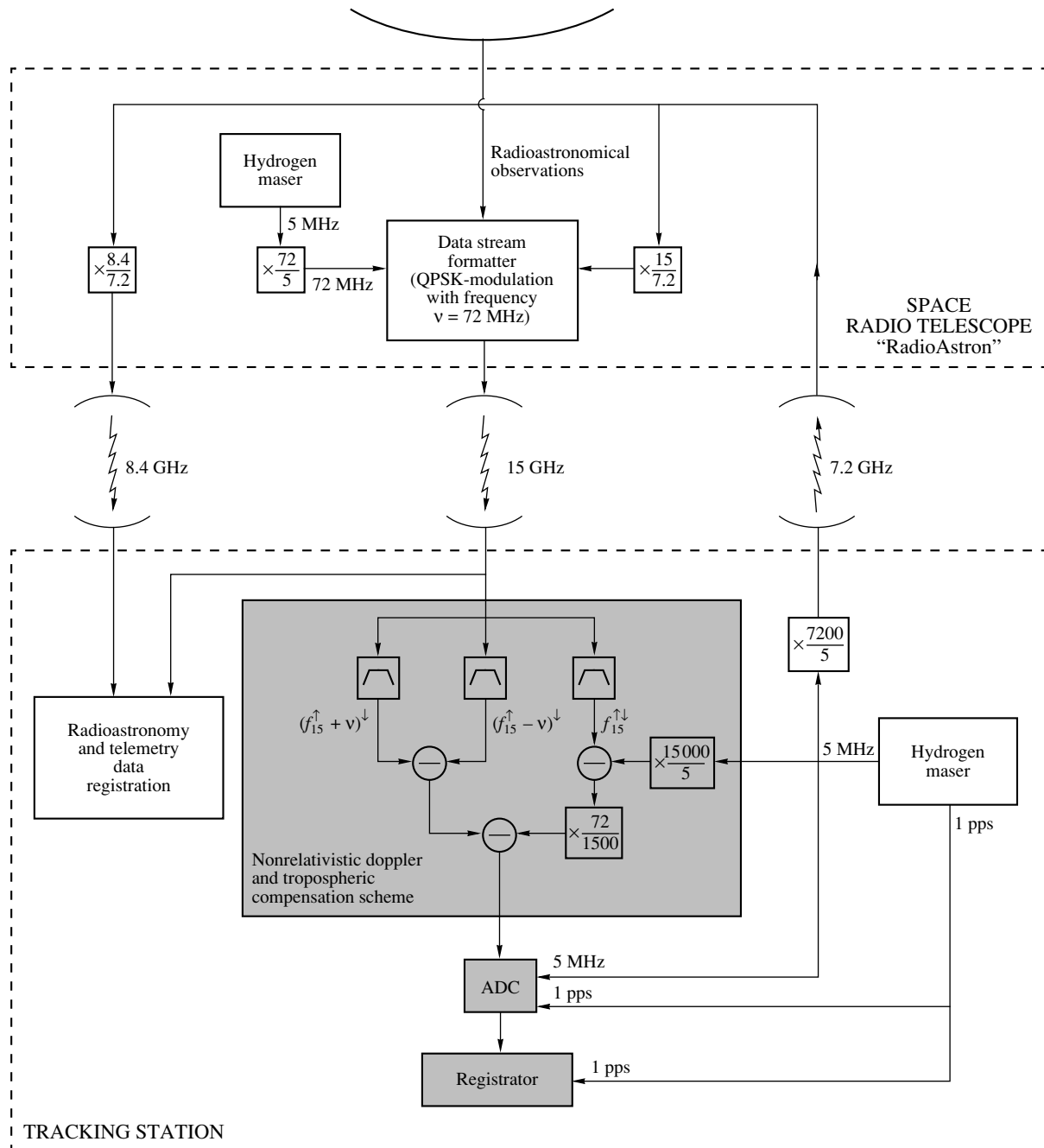


Fig. 5. Hardware approach to the nonrelativistic Doppler and tropospheric compensation.

(“Test-2”), which results in the generation of just this sequence. The spectrum of the 15 GHz signal with the formatter running the “Test-2” mode is depicted in Fig. 4.

Let us now discuss the practical means of synthesizing the signal of Eq. (29). One possible approach is to build a radio engineering hardware scheme, utilizing a set of filters, mixers, and synthesizers (Fig. 5). The input of this scheme is supplied with the 15 GHz signal from the output of the corresponding receiver of

the TS antenna. The filters select the frequency component appearing in (29) and the synthesizers and mixers perform the needed arithmetic operations. The resulting signal with frequency (34) can subsequently be fed into a frequency analyzer or recorded onto a digital media for later analysis. The other approach is to compensate offline, i.e., the 15 GHz signal is translated to an intermediate frequency, then digitized and recorded onto a media directly (by means of, e.g., VLBI-equipment). The recorded signal is sub-

sequently analyzed using optimal signal processing algorithms with the aim of determining the evolution of its spectral components in time. The frequency of Eq. (29) is synthesized in code, by applying appropriate arithmetic operations to the determined frequencies. The first method can be realized only at the TSs, while the second one can also be performed at any ground radio telescope equipped with a 2 cm receiver and a VLBI back-end (in the latter case slightly different equations have to be used).

Now Eq. (34) can be used to determine Δf_{grav} since all the other terms in it are either measurable or can be calculated from ballistic data. Let us estimate the accuracy of the SRT velocity v determination required to achieve the goal of measuring the violation parameter ε with 10^{-6} accuracy. If the SRT maximum velocity is of order 10 km/s and the error $\delta v = 3$ mm/s then $\delta \frac{v^2}{c^2} = 7 \times 10^{-16}$. The corresponding error in ε , determined in a modulation-type experiment with the available gravitational potential modulation of (21), can be found, as usual, from (11):

$$\delta\varepsilon = 1.3 \times 10^{-6}. \quad (35)$$

Therefore, the ‘‘Semi-coherent’’ mode, together with the compensation scheme (34), allows, in principle, to achieve a record accuracy of the gravitational redshift test with the available accuracy of the SRT orbit reconstruction. Note, however, that here we do not consider all the sources of error in (34) and also avoid the question of the receiving, transmitting and recording equipment noise. The results of the relevant analysis done for the GP-A scheme [15] are not fully applicable here. These matters are the subject of further research and technical tests which we are planning to give an account of later.

6. CONCLUSION

The gravitational redshift experiment is an important test of the foundations of modern physics. The currently achieved accuracy of this test with the SRT ‘‘RadioAstron’’ is $\approx 1\%$. This value can be improved considerably by using the proposed compensation scheme which requires a special mode of synchronization of the on-board radio-electronics and the high-data-rate radio complex payloads. Another requirement is for the on-board formatter to be generating a special predefined data sequence. This results in the desired properties of the signal spectrum but also makes gravitational sessions incompatible with the radio astronomical ones. The required duration of a gravitational session is ≈ 1000 s, i.e., the time interval of the best frequency stability of the SHM.

The proposed compensation scheme can be realized in two different ways. First, it can be built as

a hardware radio-electronics device from units like mixers, filters and synthesizers. This approach is possible only for the mission’s ground tracking stations. Another possibility is to record the SRT’s 15 GHz signal directly at either a TS or any ground radio telescope equipped with a 2 cm receiver and a VLBI back-end. The subsequent analysis of the recorded signal is to be performed by a purposely designed software utilizing optimal algorithms of signal parameter estimation. The advantages and drawbacks of these two approaches are the subject of the authors’ further research.

ACKNOWLEDGMENTS

The authors would like to thank N.S. Kardashev, V.V. Andreyanov, A.S. Andrianov, M.N. Andrianov, K.G. Belousov, P.A. Voitsik, B.Z. Kanevskii, Yu.Yu. Kovalev, A.V. Kovalenko, G.D. Kopelyanskii, T.A. Mizyakina, B.S. Novikov, S.V. Pilipenko, M.V. Popov, S.V. Sazankov, A.A. Skripkin, A.I. Smirnov, K.V. Sokolovskii, A.V. Chibisov, and many other colleagues from the ASC and PRAO of the LPI for their help and support in the experiment.

The ‘‘RadioAstron’’ project is led by the Astro Space Center of the Lebedev Physical Institute of the Russian Academy of Sciences and the Lavochkin Scientific and Production Association under a contract with the Russian Federal Space Agency, in collaboration with partner organizations in Russia and other countries.

REFERENCES

1. C. Misner, K. Thorne, and J. Wheeler, *Gravitation* (San Francisco: Freeman, 1973).
2. C. M. Will, *Theory and Experiment in Gravitational Physics* (Cambridge: Cambridge Univ. Press, 1993).
3. R. V. Pound and G. A. Rebka, *Phys. Rev. Lett.* **4**, 337 (1960).
4. R. V. Pound and J. L. Snider, *Phys. Rev. B* **140**, 788 (1965).
5. R. F. C. Vessot, M. W. Levine, E. M. Mattison, E. L. Blomberg, T. E. Hoffman, G. U. Nystrom, B. F. Farrel, R. Decher, P. B. Eby, C. R. Baugher, J. W. Watts, D. L. Teuber, and F. D. Wills, *Phys. Rev. Lett.* **45**, 2081 (1980).
6. M. P. Hess, L. Stringhetti, B. Hummelsberger, K. Hausner, R. Stalford, R. Nasca, L. Cacciapuoti, R. Much, S. Feltham, T. Vudali, B. Leger, F. Picard, D. Massonnet, P. Rochat, D. Goujon, W. Schaefer, P. Laurent, P. Lemonde, A. Clairon, P. Wolf, C. Salomon, I. Prochazka, U. Schreiber, and O. Montenbruck, *Acta Astron.* **69**, 929 (2011).

7. Ph. Laurent, M. Abgrall, Ch. Jentsch, P. Lemonde, G. Santarelli, A. Clairon, I. Maksimovic, S. Bize, Ch. Salomon, D. Blonde, J. F. Vega, O. Grosjean, F. Picard, M. Saccoccio, M. Chaubet, N. Ladiette, L. Guillet, I. Zenone, Ch. Delaroche, and Ch. Sirmain, *Appl. Phys. B* **84**, 683 (2006).
8. *STE-QUEST Assessment Study Report, 2013*, <http://sci.esa.int/ste-quest/53445-ste-quest-yellow-book/>.
9. N. K. Pavlis, S. A. Holmes, S. C. Kenyon, and J. K. Factor, *J. Geophys. Res. (Solid Earth)* **117**, B04406 (2012).
10. E. M. Standish, JPL Interoffice Memorandum IOM 312.F-98-048 (1998); <http://iau-comm4.jpl.nasa.gov/de405iom/de405iom.pdf>.
11. N. S. Kardashev, V. V. Khartov, V. V. Abramov, V. Yu. Avdeev, A. V. Alakoz, Yu. A. Aleksandrov, S. Ananthakrishnan, V. V. Andreyanov, A. S. Andrianov, N. M. Antonov, M. I. Artyukhov, M. Yu. Arkhipov, W. Baan, N. G. Babakin, V. E. Babyshkin, N. Bartel', K. G. Belousov, A. A. Belyaev, J. J. Berulis, B. F. Burke, A. V. Biryukov, A. E. Bubnov, M. S. Burgin, G. Busca, A. A. Bykadorov, V. S. Bychkova, V. I. Vasil'kov, K. J. Wellington, I. S. Vinogradov, R. Wietfeldt, P. A. Voitsik, A. S. Gvamichava, I. A. Girin, L. I. Gurvits, R. D. Dagkesamanskii, L. D'Addario, G. Giovannini, D. L. Jauncey, P. E. Dewdney, A. A. D'yakov, V. E. Zharov, V. I. Zhuravlev, G. S. Zaslavskii, M. V. Zakhvatkin, A. N. Zinov'ev, Yu. Ilinen, A. V. Ipatov, B. Z. Kanevskii, I. A. Knorin, J. L. Casse, K. I. Kellermann, Yu. A. Kovalev, Yu. Yu. Kovalev, A. V. Kovalenko, B. L. Kogan, R. V. Komaev, A. A. Konovalenko, G. D. Kopelyanskii, Yu. A. Korneev, V. I. Kostenko, A. N. Kotik, B. B. Kreisman, A. Yu. Kukushkin, V. F. Kulishenko, D. N. Cooper, A. M. Kut'kin, W. H. Cannon, M. G. Lariionov, M. M. Lisakov, L. N. Litvinenko, S. F. Likhachev, L. N. Likhacheva, A. P. Lobanov, S. V. Logvinenko, G. Langston, K. McCracken, S. Yu. Medvedev, M. V. Melekhin, A. V. Menderov, D. W. Murphy, T. A. Mizyakina, Yu. V. Mozgovoi, N. Ya. Nikolaev, B. S. Novikov, I. D. Novikov, V. V. Oreshko, Yu. K. Pavlenko, I. N. Pashchenko, Yu. N. Ponomarev, M. V. Popov, A. Pravin-Kumar, R. A. Preston, V. N. Pyshnov, I. A. Rakhimov, V. M. Rozhkov, J. D. Romney, P. Rocha, V. A. Rudakov, A. Räisänen, S. V. Sazankov, B. A. Sakharov, S. K. Semenov, V. A. Serebrennikov, R. T. Schilizzi, D. P. Skulachev, V. I. Slysh, A. I. Smirnov, J. G. Smith, V. A. Soglasnov, K. V. Sokolovskii, L. H. Sondaar, V. A. Stepan'yants, M. S. Turygin, S. Yu. Turygin, A. G. Tuchin, S. Urpo, S. D. Fedorchuk, A. M. Finkel'shtein, E. B. Fomalont, I. Fejes, A. N. Fomina, Yu. B. Khapin, G. S. Tsarevskii, J. A. Zensus, A. A. Chuprikov, M. V. Shatskaya, N. Ya. Shapirovskaya, A. I. Sheikhet, A. E. Shirshakov, A. Schmidt, L. A. Shnyreva, V. V. Shpilevskii, R. D. Ekers, V. E. Yakimov, *Astron. Rep.* **57**, 153 (2013).
12. R. F. C. Vessot and M. W. Levine, *Gen. Relat. and Grav.* **10**, 181 (1979).
13. A. R. Thompson, J. M. Moran, G. W. Swenson, *Interferometry and synthesis in radio astronomy* (N.-Y.: Wiley, 2001).
14. A. E. Niell, *J. Geophys. Res.* **101**, 3227 (1996).
15. R. F. C. Vessot and M. W. Levine, *NASA Experimental Final Redshift Report, GPA Project Report, Contract NAS 8-27969* (NASA, 1979).

Translated by the authors